

STRUCTURAL, THERMAL AND CONDUCTIVITY STUDIES OF PAN-LIBF₄ POLYMER ELECTROLYTES

S. K. NIPPANI^{1,*}, PIYUSH KUCHHAL¹, GAGAN ANAND¹,
VIJAY KUMAR KAMBILA²

¹Department of Physics, University of Petroleum and Energy Studies, Dehradun,
Uttarakhand, India

²Department of Physics and Nano science, KL University, Vijayawada, Andhra, India

*Corresponding Author: sknippani@gmail.com

Abstract

The polymer electrolytes with various compositions of Polyacrylonitrile/N-N Dimethylformamide (DMF)/Lithiumtetrafluoroborate (LiBF₄) are synthesized by solution casting technique. The free standing, clear and transparent 60-80 micron thick films are formed. The promising structural and complexation changes in polymer electrolytes have been explored by X-ray diffraction (XRD) and Fourier transform infra-red (FTIR) techniques. The thermal properties of all solid polymer electrolytes (SPE) were studied by Thermo gravimetric Analyzer (TGA) and Differential Thermal Analyzer (DTA). The electrical properties, i.e., ionic conductivity of solid polymer electrolytes has been measured as a function of temperature and composition. A Polymer membrane for 3 wt. % of salt has a conductivity of $3.06 \times 10^{-4} \text{ mScm}^{-1}$ at room temperature and $1.53 \times 10^{-3} \text{ mScm}^{-1}$ at 358K. The conductivity values increased with increase in temperature and offered an ionic conductivity of the order of $10^{-3} \text{ mScm}^{-1}$ at temperatures 358K. Activation energy, enthalpy and entropy values are determined for all polymer complexes.

Keywords: Solid polymer electrolyte, Polyacrylonitrile, Solution casting.

1. Introduction

Polymer Lithium ion batteries have been a significant research area for their prospective solicitations in small portable electronic and electric vehicles (EV), and personal communication equipment. Solid polymer electrolyte, used as both electrolyte and separator between the electrodes, has numerous advantages in contrast to liquid electrolyte, such as no leakage of electrolyte, ease of manufacturing, flexible geometry and improved safety, etc.

Nomenclatures

E_a	Activation energy, kJ/mol
h	Planck's constant, J s
K_B	Boltzmann constant, J/K
R	Ideal gas constant, J/mol/K
T_g	Glass transition temperature, °C
T_m	Melting temperature, °C
t_{ion}	Ionic transference number

Greek Symbols

ΔH	Enthalpy (J/mol/K)
ΔS	Entropy (J/mol/K)
ΔG	Gibb's function(kJ/mol)
λ	Wavelength (Å)
σ	Conductivity (S/m)

Abbreviations

DMF	N-N Dimethylformamide
DSC	Differential Scanning Calorimetry
DTA	Differential Thermal Analyzer
DTG	Differential Thermo grams
FIC	Fast Ion Conductors
FTIR	Fourier transform infra-red
LiBF ₄	Lithiumtetrafluoroborate
NMP	N-MethylPyrrolidine
PAN	Polyacrylonitrile
SIC	Super Ion Conductors
SPE	Solid polymer electrolytes
TG	Thermo grams
TGA	Thermo gravimetric Analyzer
XRD	X-ray diffraction

Interest in developing solid polymer electrolytes was motivated with a hope that the limitations would be minimized if the liquid electrolyte is substituted by a solid electrolyte. In thin film solid electrolytes, the lone mobile charge carrier is a cation Li^+ linked with an anion which is arrested in crystal lattice. The solid materials which exhibit high ionic conductivity comparable with those of liquid electrolytes are known as "Solid electrolytes". These materials are known as "Fast Ion Conductors (FIC)" or "Super Ion Conductors (SIC)" which are characterized by ionic bonding, high electrical conductivity ($\sim 10^{-1}$ to 10^{-4} Scm^{-1}) and ionic transport number $t_{ion} \sim 1$. In the past several years extensive studies have been performed on the ionic conductivity of certain kinds of ion conducting polymers. These ion conducting polymers show a relatively high ionic conductivity and have a potential application as solid electrolytes. Such electrolytes are mainly based on the alkali metal salt systems, with particular attention being focused on Lithium. These may be useful in finding solid electrolytes of sufficiently high conductivity.

An encouraging methodology to increase the conductivity of polymer electrolyte is through the use of low molecular weight organic solvents as

solvents or plasticizers. This method uses the smaller activation barrier for the conducting ions in the plasticizer phase than in a polymer. Furthermore, the low viscosity and high dielectric constant of these plasticizers ensures higher mobility and greater dissociation of ion pairs.

In present paper, this method is studied with various compositions of PAN/DMF/LiBF₄. The free standing, clear and transparent 60-80 micron thick films are synthesized by solution casting technique. Further, these films are put under investigation of structural, thermal and electrical properties.

2. Experimental Techniques

2.1. Synthesis of polymer electrolyte films

Polymer electrolyte films are obtained by simple casting procedure. PAN and LiBF₄ both were dried under vacuum for 4-5 hours before use so that no moisture content will be present. The weighed amounts of salt and PAN were separately dissolved in DMF and NMP respectively. During the stirring process, each flask was covered with a para film and heated up to 50°C for 24 hours approximately. Then the two solutions are mixed and further stirred at a temperature of 40°C for 24 hours until a homogeneous mixture was obtained. The homogeneous mixture was allowed to cool and was carefully put under observation for any un-dissolved, deposited or suspended particles. Then the solution was taken onto the glass petri dishes. Solvent was allowed to evaporate slowly at room temperature in a vacuum oven for a couple of weeks. Later on, the polymer film was carefully removed from the glass petri dishes without stretching and rupturing and further dried in a vacuum oven. The thickness of the cast films was observed to vary between 50 µm to 60 µm. As all these salts are highly hygroscopic, samples are stored in desiccators so as to avoid the films from the absorption of moisture. The specifications of all the films are reported in Table 1 for rest part of the paper.

Table 1. Solid Polymer electrolytes with various compositions.

Polymer Electrolyte Films	Composition
a	20:80:0
b	19:78:3
c	19:76:5
d	18:74:8
e	18:72:10
f	18:70:12

2.2. Characterization techniques

All the samples synthesized were characterized by using different experimental techniques for structural, thermal and conductivity studies. The prepared materials are characterized for spectroscopic and structural features by FTIR and X-ray diffraction respectively that are closely connected with the electronic properties.

X-ray diffractograms of different polymer electrolytes were recorded at room temperature using an X-ray powder diffractometer (Bruker D8 Advance

diffractometer) with Cu-K α radiation ($\lambda=1.5406 \text{ \AA}$). The radial scans on the SPEs were performed in terms of 2θ (Bragg angles) range ($10^\circ \leq 2\theta \leq 100^\circ$) at a scan speed of $0.5^\circ \text{ minute}^{-1}$. The infrared spectrum of polymer electrolyte films was recorded on a Perkin Elmer USA spectrum Two spectrophotometer in the wavenumber range from $450\text{-}4000 \text{ cm}^{-1}$. The experiments were performed in a dynamic nitrogen atmosphere, keeping an optical resolution of 0.2 cm^{-1} by averaging 64 scans per sample.

The TG, DTA and DTG measurements were implemented with EXSTAR TG/DTA 6300. The thermal analysis was carried out at a scanning rate of $10^\circ\text{C}/\text{min}$ in a flux of Nitrogen gas at a rate of $200\text{ml}/\text{min}$ and in the temperature range from room temperature to a maximum of 800°C . The analysis was performed by taking Alumina powder as a reference material. The ion transport is measured by using the dc polarization technique, in which a voltage of 0.5 volts was applied across the cell configuration SS|polymer electrolyte|SS and the resulting current was monitored. The temperature of the sample was controlled by varying the ac current through the heater coil of the furnace. An earthed brass sheet is placed inside the muffle furnace around the conductivity cell, so that the temperature distribution around the sample was uniform. The polarizing effects during the measurements of D.C. conductivity were minimized by applying smaller voltages for a short interval of time and short-circuiting after every reading.

3. Results and Discussion

3.1. Structural studies

XRD studies provide a perspective to identify or confirm amorphous, semi crystalline or crystalline nature of the material and the complex formation, which is vital to study about the ionic conductivity.

The diffractograms for all polymer electrolytes are reported in Fig. 1. From the diffractograms, it is observed that there is the formation of peaks at an angle of $2\theta=16.93^\circ$ to 17.46° and 29.08° to 29.6° which are in correlation with the peaks observed for pure PAN. The diffractogram of PAN powder, exhibits a reflection peaks at an angle approximately $2\theta=17^\circ$ and 29.5° corresponds to orthorhombic PAN [110] reflection with interlayer spacing, $d=5.30 \text{ \AA}$ and $d=3.05 \text{ \AA}$, respectively [1 - 3]. The XRD pattern of pure salt is taken from the standard XRD where the diffraction peaks are observed at $2\theta = 14^\circ, 21^\circ, 23^\circ, 26^\circ, 28^\circ, 32^\circ, 39^\circ, 44^\circ$ and 55° [4 - 5]. The peaks pertaining to pure salt are not present in polymer complexes as shown in Fig. 1 indicate the complete dissolution of the salt in the polymer matrix.

The crystalline regions are disturbed and there is an increase in the semi crystalline or amorphous nature in plasticized polymer electrolytes due to the addition of the salt. The diffractogram corresponding to 5 wt.% of salt concentration is broader and less prominent which confirms the semi crystalline nature [6-7]. With the addition of salt into the polymer, it is observed that the intensity of this peak is increasing and decreasing, i.e., there is a fluctuation observed in the formed peak at $2\theta=16.75^\circ$ to 17.5° . The sharp peak is becoming a broad hump or flattened in general when the salt concentration is increasing.

Figure 1 suggests the existence of multiphase systems having crystalline complexed and uncomplexed polymer along with amorphous phase [8]. Andreev [9] clearly described that the polymer electrolytes can be crystalline or amorphous, not necessarily in amorphous phase above the glass transition temperature for enhancing the ionic conductivity. Basing on the relative intensity studies from XRD patterns, it is inferred that there are no remarkable structural changes.

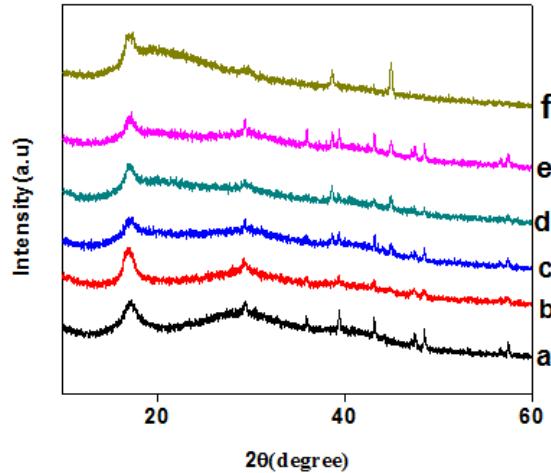


Fig. 1. X-ray diffractograms for polymer electrolytes of PAN/DMF/LiBF₄ of weight ratio (a) 20:80:0 (b) 19:78:3 (c) 19:76:5 (d) 18:74:8 (e) 18:72:10 (f) 18:70:12.

3.2. Complexation studies

Figure 2 shows the IR spectra of all the polymer electrolytes in the wavenumber from 500-4000 cm⁻¹. In the close inspection of Fig. 2, the strong bonds were observed at 1450 cm⁻¹, 1720 cm⁻¹, 2245 cm⁻¹ and 2945 cm⁻¹ for C-H bending, C=O stretching, -C≡N stretching and C-H stretching respectively for pure PAN. The C=O peak was observed at 1650 cm⁻¹ for DMF [10]. For LiBF₄, the vibrational peaks are observed at 1980 cm⁻¹, 1769 cm⁻¹ and 1545 cm⁻¹ respectively [11]. All the observed peaks are as per described in the literature.

There are quite a few ways of interaction of Li⁺ cations with -C≡N groups. (a) At least two -C≡N groups in the same polymer chain can be coordinated with Li⁺ cations or (b) The Li⁺ cations may be intermingled by -C≡N clusters of different polymer (PAN) chains or forms dissimilar micro crystallites. In these two, the former interactions are dominant as the Li⁺ cations are coordinated by the solvent molecules partially and also partially by the -C≡N groups in the same PAN Chain. In the latter, significant cross-networking effect is resulted, which results in the increase of viscosity [12].

The most prominent feature in Fig. 3 is the presence of a weak but convinced bump at 2268 cm⁻¹ on the higher frequency side of the symmetric -C≡N stretch mode observed at 2245 cm⁻¹.

This represents the interaction between the salt and the polymer. This also shows that there is no interaction between the BF_4^- anion and PAN molecules [13]. The interaction between Li^+ cations and $-\text{C}\equiv\text{N}$ group may be explained with the analysis of the chemical structure of PAN. As Li^+ cation has an empty orbital and nitrogen atom has a pair of unbound electrons, it is possible for Li^+ cation to form a bond with nitrogen atom of nitrile group to form an associate [14]. It is also observed that the intensity of the absorption band at 2245 cm^{-1} is changing (especially with the SPE with maximum concentration, which is high) on the addition of salt with increasing concentration. This clearly shows the complexation of Polyacrylonitrile with that of LiBF_4 . Appreciable change in intensity is not observed for all the SPEs. But the peak intensity is decreased for polymer electrolyte with 12wt. % concentration when compared with other polymer electrolytes [4]. At low salt concentrations, the characteristic frequency at 2269 cm^{-1} is not prominently observed. This can be attributed to the interaction between the Li^+ cation and the plasticizer decrease the bonding chance between Li^+ cation and the nitrile group of PAN [15 - 16].

Further analysis of Fig. 2 reveals that the $\text{C}=\text{O}$ stretching peak shifts from 1673 cm^{-1} to 1670 cm^{-1} with the addition of the salt and this decrease was continuous from 1670 cm^{-1} to 1660 cm^{-1} with the increase in the salt concentration from 2 wt.% to 12 wt. %. This shows the interaction of Li^+ cations with $\text{C}=\text{O}$ molecules. Further it is observed that there is a slight shift in the wavenumber around 1450 cm^{-1} which may be attributed to change in the environment of BF_4^- anions. FTIR studies show that the polymer salt complexation has taken place which is confirmed by the shifting of peaks or and also the formation of new peaks in polymer complexes. FTIR results indicate that the Li^+ cations of dissociated salt are coupled with both the $\text{C}=\text{O}$ group in DMF and the $-\text{C}\equiv\text{N}$ in PAN, along with the dipolar interactions between DMF and PAN through $\text{C}=\text{O}$ group and $-\text{C}\equiv\text{N}$.

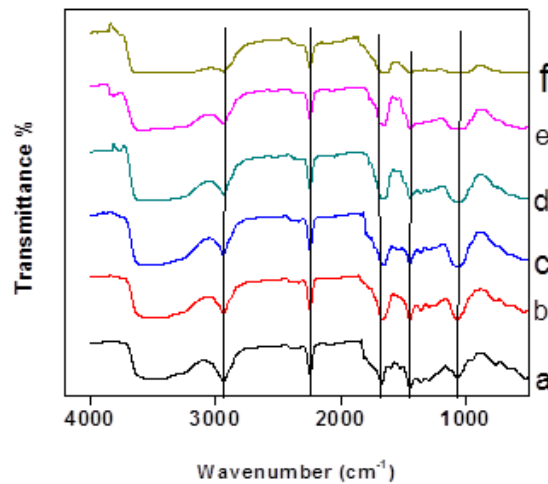


Fig. 2. IR spectra of polymer electrolytes of PAN/DMF/ LiBF_4 of weight ratio (a) 20:80:0 (b) 19:78:3 (c) 19:76:5 (d) 18:74:8 (e) 18:72:10 (f) 18:70:12.

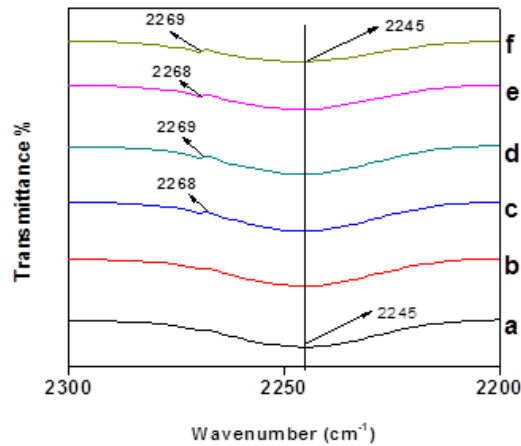


Fig. 3. IR spectra ($-C \equiv N$ stretching) of polymer electrolytes of PAN/DMF/LiBF₄ of weight ratio (a) 20:80:0 (b) 19:78:3 (c) 19:76:5 (d) 18:74:8 (e) 18:72:10 (f) 18:70:12.

3.3. Thermal studies

Thermo grams obtained for various polymer electrolytes with different doping percentage of LiBF₄ are shown in Figs. 5-7.

TGA Analysis: TG curves show that there is a gradual weight loss with temperature and it becomes 10 % when the sample reaches a temperature of 279°C when no salt is added. Further the temperature at which 10 % weight loss occurs decreases with doping concentration. This may be due to the evaporation of the solvent present in the sample.

Thermal stability is represented by determining the weight loss % of the sample after heating over temperature from 30-800 °C using TGA. From the variation in wt. % vs. temperature curves in Fig. 8, it is found that all the films are thermally stable. It is observed that there is a gradual degradation in the polymer electrolytes. All the polymer electrolytes are found to be stable up to 194, 138, 89, 91 and 91°C which imply that the films exhibit good thermal stability. The Residue or the Characteristic Yield is decreasing at temperatures approximately at around 800 °C.

DTA Analysis: From DTA curves in Fig. 6, it is difficult to observe the crystallinity peak because the crystalline hump will be formed well before the melting peak. If crystallinity is present then there could have been the formation of the peak in the downward (exo) direction, which is not observed in DTA curves.

As the crystalline peak is not observed and it is not amorphous, the host material is found to be semi crystalline in nature which is even confirmed from the XRD studies. The temperature at which the last bond of the polymer structure breaks is called as the melting temperature (T_m). The melting temperature of the polymer complex without salt is decreased from the standard value of 317 °C to 279 °C. The melting temperature of the polymer electrolytes is further decreased with the addition of salt into the polymer. The addition of salt may be helping the decomposition process and may be activating the degradation, which infers that

the thermal stability is decreasing as inferred from TGA, in turn implies that the thermal conductivity will also decrease accordingly.

The Glass transition temperature can be defined from DTA, but can be measured much more precisely from DSC. Pure PAN exhibits a glass transition temperature of 88.1°C [17]. It is observed from DTA curves that the glass transition temperature of the cast film decreased for the host polymer. It is observed that the glass transition temperature of the polymer- salt complexes decreases with the introduction of salt. This may be due to the presence of the plasticizer and interaction of plasticizer with the salt. The spacing of Nitrile groups decreases dipolar interactions which increases the free volume which intern decreases the glass transition temperature. When salt concentration is further increased, the glass transition temperature is increased from 55-70 °C for concentrations from 5 wt. % to 12 wt. % of salt. The increase in glass transition temperature with increasing salt content indicates the decrease in free volume of the material [18]. With increase in salt doping percentage, T_g is increased which shows that the crystallinity of the complexes is increasing confirmed from XRD as well. DTG curves in Fig. 7 reveals the same result as DTA.

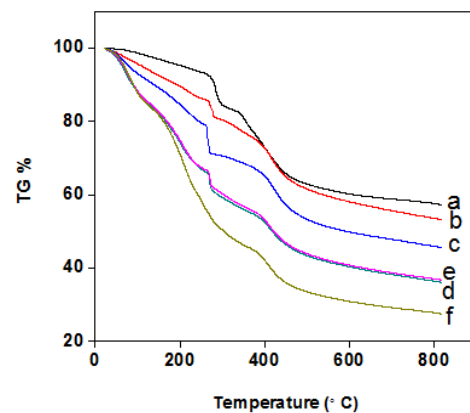


Fig. 5. TG curves for polymer electrolytes of PAN/DMF/LiBF₄ of weight ratio (a) 20:80:0 (b) 19:78:3 (c) 19:76:5 (d) 18:74:8 (e) 18:72:10 (f) 18:70:12.

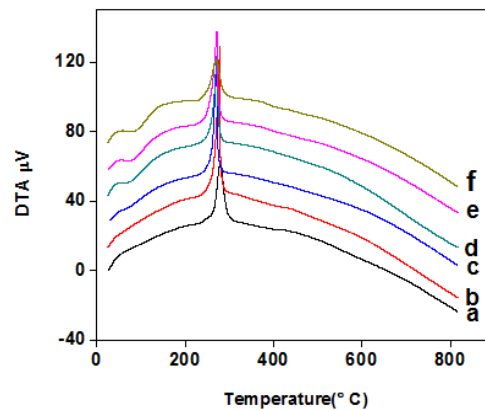


Fig. 6. DTA curves for polymer electrolytes of PAN/DMF/LiBF₄ of weight ratio (a) 20:80:0 (b) 19:78:3 (c) 19:76:5 (d) 18:74:8 (e) 18:72:10 (f) 18:70:12.

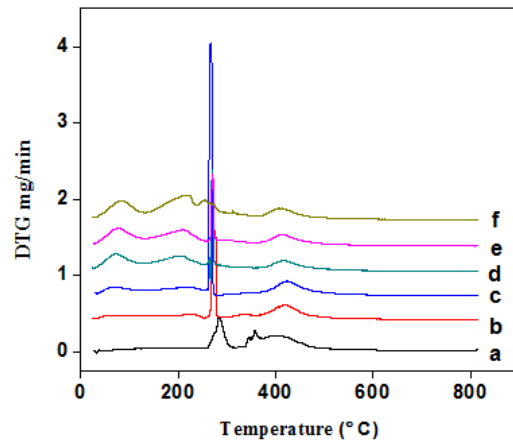


Fig. 7. Extended DTG curves for polymer electrolytes of PAN/DMF/LiBF₄ of weight ratio (a) 20:80:0 (b) 19:78:3 (c) 19:76:5 (d) 18:74:8 (e) 18:72:10 (f) 18:70:12.

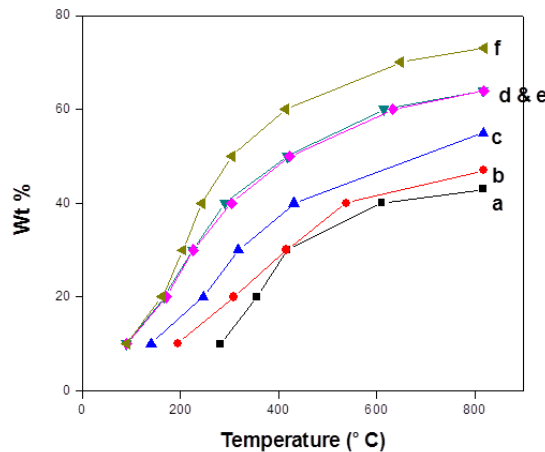


Fig. 8. Yield percentages from TG curves for polymer electrolytes of PAN/DMF/LiBF₄ of weight ratio (a) 20:80:0 (b) 19:78:3 (c) 19:76:5 (d) 18:74:8 (e) 18:72:10 (f) 18:70:12.

3.4. Conductivity studies

The ionic conductivities of SPEs as a function of different wt. % of salt over the temperature 313-358 K are shown in Fig. 9.

3.4.1. Concentration dependent conductivity

The conductivity of the pure PAN at room temperature is of the order of 10^{-11} Scm^{-1} [14]. When the LiBF₄ is added, most of the salt gets dissociated, due to which the order of the conductivity increases to 10^{-7} Scm^{-1} . The probable reason

for low conductivity is that most of the dissolved Li^+ ions coordinate to the oxygen in the carbonyl group in DMF as clear from FTIR studies. This result may be due to the formation of a cross link between the chain segments which reduce the mobility of the charge carriers and tend to decrease the conductivity [19 - 20]. Fig. 9 witnessed that the conductivity is increasing as concentration of salt increases. At 313 K, it is observed that the conductivity increased from $3.05 \times 10^{-4} \text{ mScm}^{-1}$ for 3 wt. % to $4.43 \times 10^{-4} \text{ mScm}^{-1}$ for 12 wt. % of LiBF_4 . The conductivity increases even when the free volume decreases as confirmed from FTIR studies. The increase in conductivity with salt concentration may be ascribed to the solvation of Lithium salts to produce free ions which increases conductivity but tends to increase T_g by immobilization of chain segments. An ionic-cross-link network is assumed where the cross link density increases with salt concentration [21]. It is also found that the polymer salt complexes start melting at around 270°C which is in agreement with the results from TGA.

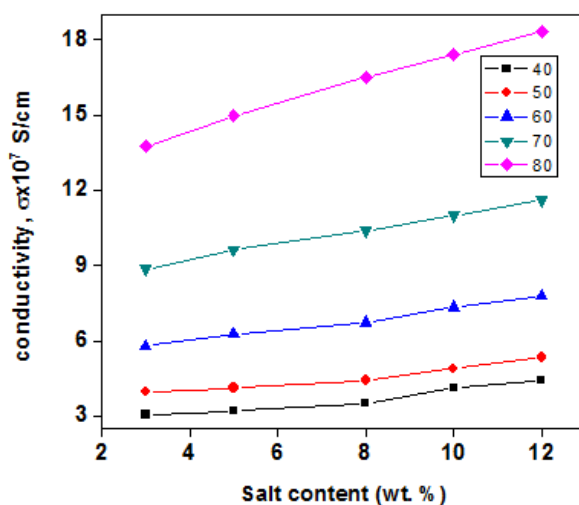


Fig. 9. Variation between conductivity vs. wt. % of LiBF_4 content in polymer electrolytes of PAN/DMF/ LiBF_4 at different temperatures.

3.4.2. Temperature dependent ionic conductivity

The temperature variations of conductivity are shown in Fig. 10. It is observed that the curves follow the Arrhenius relation for ion transport, i.e., the major ions movement happen by an activated hopping, decoupled with the polymer matrix at elevated temperatures. In addition to above mechanism, the ionic conductivity of a SPE increases with temperature is due to the higher segmental motion of the polymer chain [15 - 16] which is in the semi-crystalline phase as confirmed from the XRD studies. Also, the higher conductivity at elevated temperatures may be due to the motion of Li^+ along the segmental chain. The appearance of shoulder near to 2260 cm^{-1} in FTIR indicates the coordination of some Li^+ with $-\text{C}\equiv\text{N}$ of PAN which contributes in conductivity through segmental chain motion which is more prominent at high temperatures. When the temperatures are approaching towards the higher side, i.e., at 358 K, the

conductivity values increased from $1.52 \times 10^{-3} \text{ mScm}^{-1}$ for 3 Wt.% to $2.14 \times 10^{-3} \text{ mScm}^{-1}$ for 12 wt. % of LiBF₄.

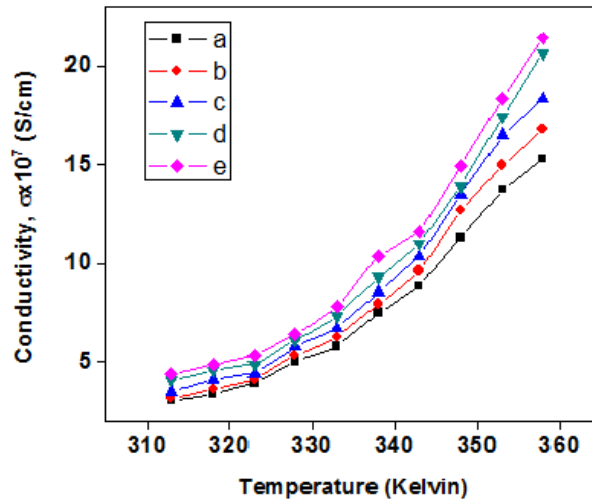


Fig. 10. Arrhenius plot of ionic conductivity vs. Temperature for polymer electrolytes of PAN/DMF/LiBF₄ of weight ratio (a) 19:78:3 (b) 19:76:5 (c) 18:74:8 (d) 18:72:10 (e) 18:70:12.

3.4.3. Activated properties of solid polymer electrolytes

The temperature dependent conductivity for all polymer electrolytes may be given by the Arrhenius type relation given by Eq. (1).

$$\sigma(T) = A \exp\left(\frac{-E_a}{KT}\right) \quad (1)$$

where 'A' is the pre-exponential factor, proportional to the number of carrier ions, 'E_a' is the activation energy for electrical conduction (energy required for an ion to jump to a free hole). If conductivity is result of thermal activation process, Enthalpy (ΔH) and Entropy (ΔS) are determined from the Eyring equation, a linear relation obtained as a plot of $\ln(\sigma h / K_B T)$ vs $1000/T$, given by Eq. (2).

$$R \ln\left(\frac{\sigma h}{K_B T}\right) = -\left(\frac{\Delta H}{T}\right) + \Delta S \quad (2)$$

where "h" is the Planck's constant and "K_B" is the Boltzmann constant.

The another general linear form of Arrhenius-like expression is given by Eyring-Polanyi equation, that relates the conductivity with the Gibb's function to determine the values of Enthalpy (ΔH) and Entropy (ΔS), given by Eq. (3).

$$\sigma = \left(\frac{K_B T}{h}\right) \exp\left(\frac{-\Delta G}{RT}\right) \quad (3)$$

This can be written in the form of $y=mx+c$ as given by Eq. (4).

$$\ln\left(\frac{\sigma}{T}\right) = -\left(\frac{\Delta H}{RT}\right) + \left(\frac{\Delta S}{R}\right) + \ln\left(\frac{K_B}{h}\right) \quad (4)$$

where slope determines enthalpy of activation, $-\Delta H(m= -\Delta H/R)$ and the intercept gives entropy of activation, $\Delta S[\text{Intercept} = (\Delta S/R) + \ln(k/h)]$.

The values of activation energy are calculated from the linear plots of $10^3/T$ vs $\ln \sigma$. The activation energy values decreased from 34.05 KJ/mole 3 Wt.% to 32.45 for 12 wt. % of LiBF_4 . Enthalpy and Entropy values are determined from linear plots of $10^3/T$ vs $\ln(\sigma/T)$. The enthalpy values decreased from 31.22 J/mol/K for 3 wt.% to 29.61 J/mol/K for 12 wt.%. The entropy values changed from -270.91 J/mol/K for 3wt.% to -273.19 J/mol/K for 12 wt.%. It is observed that there is an increase in conductivity and decrease in activation energy with the increase in dopant concentration. This can be explained basing on the mixed phases, either amorphous or semi-crystalline nature present in polymer films. The result illustrates that the conductivity in such films may be dominated by the amorphous phase which may be due to the formation of charge complexes in the host lattice [22]. These charge transfer complexes increase the additional charges in the lattice which results in an increase in conductivity and decrease in activation energy [23].

4. Conclusions

The structural, complexation, thermal and conductivity properties of the polymer electrolytes were studied. The structural studies from XRD reveals about the semi crystalline nature of the polymer electrolytes. The complexation confrontation was confirmed from FTIR basing on the shifting of the peaks that confirms the interactions. The thermal properties provide the strong evidences about the thermal stability and the degradation of the polymer electrolytes. The concentration and temperature dependent ionic conductivity values of the polymer electrolytes so found were of low values but increasing with salt concentration and temperature as well. It is also observed that the values of activation energy, enthalpy and entropy were decreased with the increase of salt concentration. The low results are mainly due to the low concentration of the salt employed in the synthesis process.

Acknowledgements

I sincerely thank the UPES management for sanctioning the financial aid to carry out the work.

References

1. Sawai, D.; Miyamoto, M.; Kanamoto, T.; and Ito. M. (2000). Lamellar thickening in nascent poly(acrylonitrile) upon annealing. *Journal of Polymer Science Part B: Polymer Physics*, 38(19), 2571-2579.
2. Rajendran, S.; Kannan, R; and Mahendran, O. (2001). Study on Li ion conduction behaviour of the plasticized polymer electrolytes based on poly acrylonitrile. *Materials Letters*, 48(6), 331-335.

3. Zhang, Z.; Zhang, L.; Wang, S.; Chen, W; and Lei, Y. (2001). A convenient route to polyacrylonitrile/silver nanoparticle composite by simultaneous polymerization-reduction approach. *Polymer*, 42(19), 8315-8318.
4. Ahmad, A.; Md. Isa, K.B.; and Osman, Z. (2011). Conductivity and structural studies of plasticized polyacrylonitrile (PAN) - lithium triflate polymer electrolyte films. *Sains Malaysiana*, 40(7), 691-694.
5. Fahmi, E.M.; Ahmad, A.; Nazeri, N.N.M.; Hamzah, H.; Razali, H.; and Rahman, M.Y.A. (2012). Effect of LiBF₄ salt concentration on the properties of poly(ethylene oxide)-based composite polymer electrolyte. *International Journal of Electrochemical Science*, 7(8), 5798-5804.
6. Hodge, R.M.; Edward, G.H.; and Simon., G.P. (1996). Water absorption and states of water in semicrystalline poly(vinyl alcohol) films. *Polymer*, 37(8), 1371-1376.
7. Helan Flora, X.; Ulaganathan, M.; and Rajendran, S. (2012). Influence of lithium salt concentration on PAN-PMMA blend polymer electrolytes. *International Journal of Electrochemical Science*, 7(8), 7451-7462.
8. Subban, R.H.Y.; and Arof, A.K. (2003). Experimental investigations on PVC-LiCF₃SO₃-SiO₂ composite polymer electrolytes. *Journal of New Materials for Electrochemical Systems*, 6(6), 197-203.
9. Andreev, Y.G.; Seneviratne, V.; Khan, M.; Henderson, W.A.; Frech, R.E.; and Bruce., P.G. (2005). Crystal structures of poly(ethylene oxide)₃:LiBF₄ and (Diglyme)_n:LiBF₄ (n = 1,2). *Chemistry of Materials*, 17(4), 767-772.
10. Kim, Y.J.; and Park, C.R. (2005). The effect of the interaction between transition metal and precursor on the stabilization reaction of polyacrylonitrile (PAN). *Carbon*, 43(11), 2420-2423.
11. Ramesh Prabhu, M.; Sudalaimuthu, K.; and Rajendran, S. (2013). Investigations on PVC/PMMA blends with various lithium salts. *Paripex, Indian Journal of Research*, 2(3), 307-309.
12. Park, U.S.; Hong, Y.J.; and Oh, S.M. (1996). Fluorescence spectroscopy for local viscosity measurements in polyacrylonitrile (pan)-based polymer gel electrolytes. *Electrochimica Acta*, 41(6), 849-855.
13. Huang, B.; Wang, Z.; Chen, L.; Xue, R.; and Wang., F. (1996). The mechanism of lithium ion transport in polyacrylonitrile-based polymer electrolytes. *Solid State Ionics*, 91(3-4), 279-284.
14. Wang, Z.; Huang, B.; Xue, R.; Huang, X.; and Chen., L. (1999). Spectroscopic investigation of interactions among components and ion transport mechanism in polyacrylonitrile based electrolytes. *Solid State Ionics*, 121(1-4), 141-156.
15. Kuo, C.W.; Huang, C.W.; Chen, B.K.; Li, W.B.; Chen, P.R.; Ho, T.H.; Tseng, C.G.; and Wu., T.Y. (2013). Enhanced ionic conductivity in PAN-PEGME-LiClO₄-PC composite polymer electrolytes. *International Journal of Electrochemical Science*, 8(3), 3834-3850.
16. Kuo, C.W.; Li, W.B.; Chen, P.R.; Liao, J.W.; Tseng, C.G.; and Wu., T.Y. (2013). Effect of plasticizer and lithium salt concentration in PMMA-based composite polymer electrolytes. *International Journal of Electrochemical Science*, 8(4), 5007-5021.

17. Jayathilakaa, P.A.R.D.; Dissanayakea, M.A.K.L.; Albinssona, I.; and Mellander, B.E. (2003). Dielectric relaxation, ionic conductivity and thermal studies of the gel polymer electrolyte system PAN/EC/PC/LiTFSI. *Solid State Ionics*, 156(1-2), 179-195.
18. Chen-Yang, Y.W.; Chen, H.C.; Lin, F.J.; and Chen, C.C. (2002). Polyacrylonitrile electrolytes: A novel high-conductivity composite polymer electrolyte based on PAN, LiClO₄ and α -Al₂O₃. *Solid State Ionics*, 150(3-4), 327-335.
19. Othman, L.; Chew, K.W.; and Osman, Z. (2007). Impedance spectroscopy studies of poly (methyl methacrylate)-lithium salts polymer electrolyte systems. *Ionics*, 13(5), 337-342.
20. Ali, A.M.M.; Subban, R.H.Y.; Bahron, H.; Winie, T.; Latif, F.; and Yahya, M.Z.A. (2008). Grafted natural rubber-based polymer electrolytes: ATR-FTIR and conductivity studies. *Ionics*, 14(6), 491-500.
21. Watanabe, M.; Kanba, M.; Nagaoka, K.; and Shinohara, I. (1983). Ionic conductivity of hybrid films composed of polyacrylonitrile, ethylene carbonate, and LiClO₄. *Journal of Polymer Science: Polymer Physics Edition*, 21(6), 939-948.
22. Ramu, C.; Naidu, Y.R.V.; and Sharma, A.K. (1994). Dielectric relaxation in iodine doped cellulose acetate films. *Ferroelectrics*, 159(1), 275-280.
23. Chandra Sekhar, P.; Naveen Kumar, P.; and Sharma, A.K. (2012). Role of salt concentration on conductivity and discharge characteristics of PMMA based polymer electrolyte system. *International Journal of Scientific and Research Publications*, 2(12), 1-5.